THE JOURNAL OF PHYSICAL CHEMISTRY B LETTERS

2006, *110,* 4531−4534
Published on Web 02/18/2006

DFT-Based Prediction of High-Pressure H_2 Adsorption on Porous Carbons at Ambient Temperatures from Low-Pressure Adsorption Data Measured at 77 K

Jacek Jagiello,*,† Alejandro Ansón,‡ and M. Teresa Martínez‡

Quantachrome Instruments, 1900 Corporate Drive, Boynton Beach, Florida 33426, and Instituto de Carboquímica, CSIC, C/Miguel Luesma Castán, 4, 50018 Zaragoza, Spain

Received: December 15, 2005; In Final Form: February 1, 2006

Hydrogen adsorption isotherms were measured both at cryogenic temperatures below 1 atm and at ambient temperature at high pressures, up to 90 atm, on selected porous carbons with various pore structures. The nonlocal density functional theory (NLDFT) model was used to calculate the pore size distributions (PSDs) of the carbons, from H_2 adsorption isotherms measured at 77 K, and then to predict H_2 adsorption on these carbons at 87 and 298 K. An excellent agreement between the predicted and measured data was obtained. Prior to analyzing the porous carbons, the solid−fluid interaction parameters used in the NLDFT model were derived from H_2 adsorption data measured at 77 K on nonporous carbon black. The results show that the NLDFT model with appropriate parameters may be a useful tool for optimizing carbon pore structures and designing adsorption systems for hydrogen storage applications.

Introduction

Application of hydrogen as a clean fuel for automotive applications requires the solution of several fundamental and practical problems. Safe and convenient storage of hydrogen is one of the main challenges that need to be solved. Storage by means of physical adsorption on various microporous materials is being considered as one of the solutions.[1,2] Among the most often studied candidates for such applications are activated carbons,[3−5] synthetic carbons,[6] single- and multiwalled nanotubes,[7,8] and metal organic framework materials.[9,10] To develop materials of practical significance for hydrogen storage, it is important to understand the relationship between pore structure and hydrogen adsorption capacity under various temperature and pressure conditions. Traditionally, the pore structure of porous materials has been described in terms of pore size distribution (PSD), evaluated from the analysis of nitrogen or argon adsorption isotherms measured at cryogenic temperatures.[11] Recently, successful predictions of adsorption of supercritical gases other than H_2 on activated carbons were obtained using the nonlocal density functional theory (NLDFT)[12] and finite pore wall thickness model.[13] The predictions were based on PSD data derived from Ar adsorption isotherms at 87 K. For the prediction of H_2 adsorption, however, it is sensible to also use H_2 data for carbon characterization.[14] This is because the fraction of the pores accessible to H_2 may not be accessible to N_2 or Ar, especially at cryogenic temperatures.

The purpose of this work is to demonstrate that H_2 adsorption data measured at cryogenic temperatures below 1 atm can be used for prediction of high-pressure H_2 adsorption at ambient temperatures, the conditions of practical storage applications. The prediction procedure employs model adsorption data calculated using the NLDFT. In this work, the NLDFT model is first used to calculate the PSD for a given carbon from its H_2 adsorption data measured at 77 K and then to calculate adsorption for that carbon at 87 and 298 K. A good agreement between predicted and experimental data was obtained for three carbons representing different pore structures.

Experimental Section

A nonporous graphitized carbon black, Carbopack F (Supelco), and three porous carbon samples, Carbosieve S (Supelco), Maxsorb (Kansai Coke & Chemicals), and Norit, representing different pore structures were selected for this study. Measurements of Ar, N_2, and H_2 adsorption at cryogenic temperatures (77.3 and 87.4 K) were performed in the pressure range 0.001−760 Torr using an Autosorb 1 MP (Quantachrome Instruments). High-pressure H_2 isotherms were measured at 298 K using a GHP-SF gravimetric adsorption analyzer (VTI Corporation) equipped with a magnetic suspension system (Rubotherm GmbH). The sample volume was evaluated by helium displacement, and buoyancy correction was calculated using the Peng−Robinson equation of state.[15] Samples of about 70 mg and 700−800 mg were used for low- and high-pressure measurements, respectively. Prior to the adsorption measurements, the samples were outgassed for 12 h at 580 K under high vacuum.

Results and Discussion

In this work, the calculations of model H_2 isotherms were performed following the implementation of Tarazona's NLDFT[12] described by Lastoskie et al.[16] The slit pore model was assumed for carbon pores, and the carbon−fluid interactions were described by the Steele potential.[17] Because at low

* Corresponding author's email address: jacek.jagiello@quantachrome.com.
† Quantachrome Instruments.
‡ Instituto de Carboquímica.

10.1021/jp057340x CCC: $33.50 © 2006 American Chemical Society

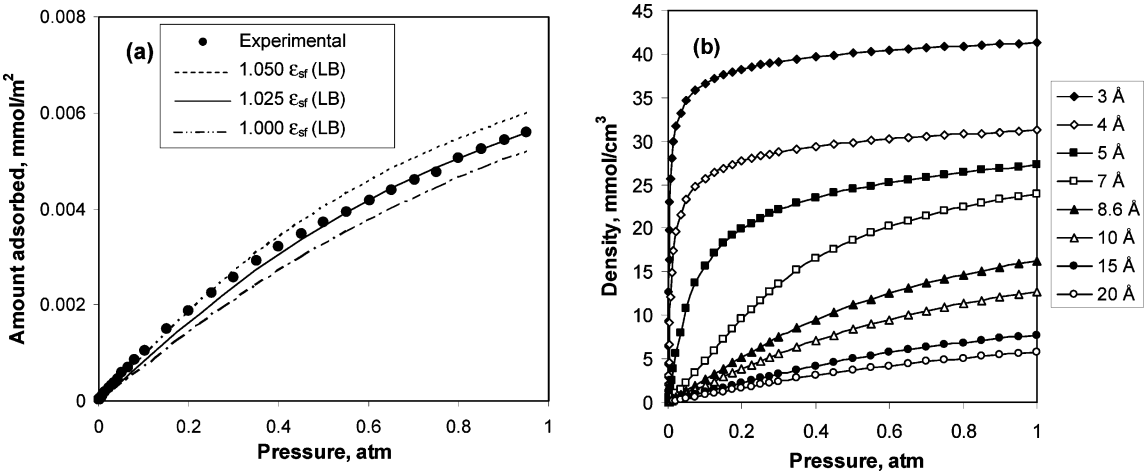

Figure 1. (a) Model H_2 adsorption isotherms at 77 K calculated for flat carbon surface with different values of the interaction parameter ϵ_{sf} compared to experimental data measured on graphitized carbon black. (b) Model H_2 isotherms at 77 K expressed as densities inside the pores for selected pore widths.

TABLE 1: Parameters Used for the NLDFT Calculations of H_2 Model Isotherms (kernels)

parameter	σ_{ff} Å	ϵ_{ff}/k K	σ_{sf} Å	ϵ_{sf}/k K
value	3.04	34.3	3.22	31.8

temperatures H_2 is a quantum fluid, the quantum corrections were applied in all NLDFT calculations by using Feynman's "effective potential".[18] The Lennard-Jones fluid−fluid interaction parameters ϵ_{ff} and σ_{ff} for H_2 were taken from Stan and Cole[18] who derived them from the Silvera−Goldman[19] potential. For the H_2 hard-sphere diameter, the value of σ_{ff} was used. An initial approximation for the carbon−H_2 interaction parameters was obtained by applying the Lorentz−Berthelot (LB) combining rules.[17] Using these parameters, we calculated the NLDFT adsorption isotherm of H_2 on the model flat carbon surface at 77 K and compared it with the H_2 isotherm (Figure 1a) measured at the same temperature on the nonporous and energetically homogeneous[20] carbon Carbopack, whose surface area of 6.4 m^2/g was determined by the *t*-plot method from the N_2 isotherm using the de Boer's *t*-curve.[21] As Figure 1a shows, the theoretical isotherm calculated using the LB derived parameters slightly underestimates the experimental data. To improve the agreement between the model and the experiment, we adjusted the solid−fluid interaction parameter ϵ_{sf} and found that the best fit is achieved for the value of this parameter, which is approximately 2.5% larger than the ϵ_{sf}(LB) value derived from the LB rule. The values of parameters used in our calculations of model H_2 adsorption isotherms are summarized in Table 1.

We calculated three sets (kernels) of model NLDFT isotherms of H_2 adsorption at three temperatures, 77.3, 87.4, and 298 K. The kernels for cryogenic and ambient temperatures were calculated for pressure ranges 0−1 and 0−100 atm, respectively. Figure 1b shows selected model H_2 isotherms at 77 K calculated for several pore widths. The pore width, *w*, is considered here an "effective pore width"[22] defined as $w = H - 3.4$ Å, where *H* is the distance between the centers of the surface carbon atoms in the opposite pore walls. The isotherms in Figure 1b are expressed in terms of the H_2 density calculated per effective pore volume.

It is interesting to note that the calculated density of H_2 at 1 atm and 77 K in the 3 Å pore is about 0.08 g/cm^3, which is higher than its liquid density of 0.07 g/cm^3 at the boiling point. Such a high density of H_2 is achieved in the carbon pores that can accommodate only a single layer of H_2 molecules because

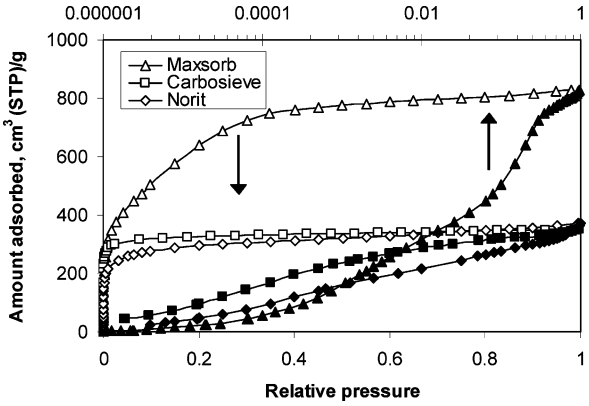

Figure 2. Experimental argon adsorption isotherms measured at 87 K on Maxsorb (triangles), Carbosieve (squares), and Norit (diamonds) samples plotted in linear (bottom scale, white symbols) and logarithmic (top scale, black symbols) pressure scales.

of the strong solid−fluid interaction potential exhibited by the pore walls, which are in very close proximity to each other. A similar value of H_2 density at 1 atm and 77 K in the carbon slit pores of similar sizes can be deduced from the results reported by Wang and Johnson,[23] who simulated the H_2 adsorption in the carbon pores using the grand canonical Monte Carlo simulations combined with the path integral method which accounts for quantum effects.

Adsorption properties of carbon samples selected for this study are illustrated by argon (Figure 2) and hydrogen (Figure 3a) adsorption isotherms measured at 87 and 77 K, respectively. Standard characteristics of these samples, obtained from Ar isotherms, and their H_2 adsorption capacities measured at 1 atm and 77 K are collected in Table 2. It is interesting to note that the H_2 adsorption capacities of these samples are correlated neither with BET surface areas nor with DR micropore volumes. Clearly, the Maxsorb sample adsorbs significantly less H_2 than Carbosieve, even though the values of its surface area and micropore volume are more than 60% higher than those for Carbosieve sample. On the other hand, it appears that H_2 adsorption isotherms (Figure 3a) show a similar trend to Ar isotherms (Figure 2) in the range of low relative pressures (<0.01) corresponding to adsorption in small micropores. These observations can be explained by the fact that at 77 K and 1 atm the studied carbon materials are far from their saturation limits for H_2 adsorption, and the H_2 molecules

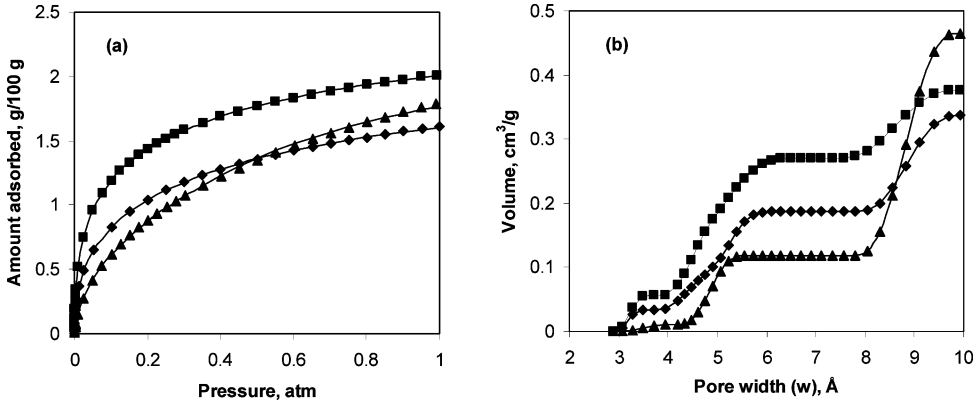

Figure 3. Hydrogen adsorption results for Maxsorb (triangles), Carbosieve (squares), and Norit (diamonds) samples. (a) Experimental H_2 adsorption isotherms at 77 K (solid symbols) and their fits by eq 1 (continuous lines). (b) Calculated cumulative pore size distributions.

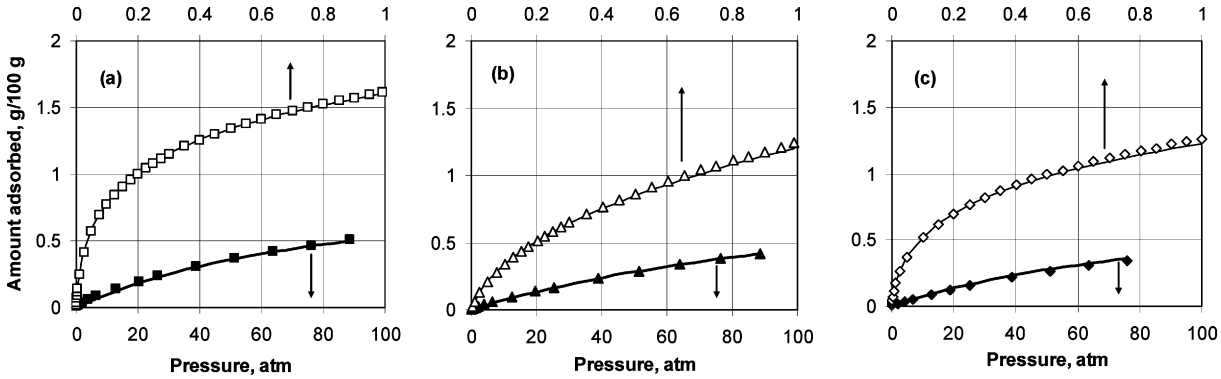

Figure 4. Excess H_2 adsorption isotherms for Carbosieve (a), Maxsorb (b), and Norit (c) samples. Experimental data are shown as white (for 87 K) and black symbols (for 298 K). Results of prediction are shown as continuous thin (for 87 K) and thick (for 298 K) lines. Top and bottom pressure scales refer to 87 and 298 K data, respectively.

TABLE 2: Basic Characteristics of Carbon Samples Derived from Adsorption Isotherms of Ar at 87 K and H_2 at 77 K

sample	BET_{Ar} surface area m^2/g	DR_{Ar} micropore volume cm^3/g	H_2 adsorption at 1 atm g/100 g
Maxsorb	2100	0.69	1.8
Carbosieve	1120	0.42	2.0
Norit	970	0.38	1.6

are predominantly adsorbed in the range of the smallest pores where the adsorption energies are the highest.

To obtain a more accurate description of the carbon capacity for H_2 adsorption in a wide range of temperatures and pressures, we employ the NLDFT model discussed above. First, we calculate the PSDs of the carbons from their H_2 adsorption isotherms measured at 77 K using the appropriate NLDFT kernel. The PSD is calculated by solving the adsorption integral equation

$$V(p) = \int [\rho(p, w) - \rho_g(p)]\, f(w)\, dw \qquad (1)$$

where $V(p)$ is the experimental excess isotherm, ρ_g is the gas bulk density, and $\rho(p, w)$ is the kernel given in terms of the adsorbate density calculated for model pores as a function of pore width, w, and equilibrium pressure, p. The PSD to be determined is represented as a differential pore volume distribution, $f(w)$. To obtain a stable and physically feasible solution for $f(w)$, we use the numerical algorithm SAIEUS,[24] which utilizes the regularization procedure and imposes nonnegativity constraints on the solution.[24,25] The results of fitting eq 1 to the experimental H_2 isotherms and the calculated cumulative PSDs are shown in Figure 3. Because H_2 isotherms at 77 K are only sensitive to pore sizes of very small pores and become linearly dependent for pores larger than ~10 Å (see Figure 1b), we calculated carbon PSDs assuming 10 Å as the upper limit of the integral in eq 1. The assumed integration range is additionally supported by the recent experimental study[6] which demonstrated that carbon pores in this range are the most efficient for H_2 adsorption at 77 K below 1 atm.

The PSDs calculated from the 77 K isotherms can now be used in conjunction with the appropriate kernels as input data in eq 1 to predict excess adsorption at other temperatures. Figure 4 shows such predicted isotherms at 87 and 298 K for the three studied carbon samples. It is seen that in all cases excellent agreement was obtained between the experimental and predicted adsorption isotherms. These results show that the information about the carbon pore structure extracted from the H_2 adsorption isotherm measured at 77 K below 1 atm is sufficient to accurately describe the H_2 adsorption on that carbon in a wide range of temperatures and pressures.

It is important to note that the absolute adsorption amount, which is related to gas storage capacity, is simply obtained from the excess amount by adding the amount of bulk H_2 gas that fills the carbon pore volume at a given temperature and pressure. The ability to model hydrogen storage capacity in the range of temperatures and pressures corresponding to conditions of practical storage applications may be very useful for optimizing carbon pore structures and designing hydrogen storage systems.

Conclusions

We have demonstrated that the NLDFT model for H_2 adsorption in carbon pores may quantitatively predict high-pressure hydrogen adsorption and storage on porous carbons at

ambient temperatures from H_2 adsorption measurements at cryogenic temperatures below 1 atm. The important part of our approach is the evaluation of carbon PSD for the range of pore sizes that are most effective for H_2 adsorption. We chose H_2, instead of standard N_2, for the PSD calculation because some of the small pores accessible to H_2 may not be accessible to N_2 or Ar molecules. We find that using the PSD in the range below 10 Å is sufficient to accurately describe H_2 adsorption on the porous carbon at low temperatures and pressures as well as at high temperatures and pressures.

Acknowledgment. We thank Dr. William R. Betz, Supelco, Inc., for selecting and providing carbon samples.

References and Notes

(1) Schlapbach, L.; Zuttel, A. *Nature (London)* **2001**, *414*, 353−358.
(2) Zhou, L. *Renewable Sustainable Energy Rev.* **2005**, *9*, 395−408.
(3) Amankwah, K. A. G.; Noh, J. S.; Schwarz, J. A. *Int. J. Hydrogen Energy* **1989**, 437−447.
(4) de la Casa-Lillo, M. A.; Lamari-Darkrim, F.; Cazorla-Amoros, D.; Linares-Solano, A. *J. Phys. Chem. B* **2002**, *106*, 10930−10934.
(5) Benard, P.; Chahine, R. *Langmuir* **2001**, *17*, 1950−1955.
(6) Gogotsi, Y.; Dash, R. K.; Yushin, G.; Yildirim, T.; Laudisio, G.; Fischer, J. E. *J. Am. Chem. Soc.* **2005**, *127*, 16006−16007.
(7) Cheng, H.-M.; Yang, Q.-H.; Liu, C. *Carbon* **2001**, *39*, 1447−1454.
(8) Anson, A.; Jagiello, J.; Parra, J. B.; Sanjuan, M. L.; Benito, A. M.; Maser, W. K.; Martínez, M. T. *J. Phys. Chem. B* **2004**, *108*, 15820−15826.
(9) Rowsell, J. L. C.; Yaghi, O. M. *Angew. Chem., Int. Ed.* **2005**, *44*, 4670−4679.
(10) Lee, J. Y.; Pan, L.; Kelly, S. P.; Jagiello, J.; Emge, T. J.; Li, J. *Adv. Mater.* **2005**, *17*, 2703−2706.
(11) Gregg, S. J.; Sing, K. S. W. *Adsorption, Surface Area and Porosity*; Academic Press: London, 1982.
(12) Tarazona, P.; Marini Bettolo Marconi, U.; Evans, R. *Mol. Phys.* **1987**, *60*, 573−595.
(13) Nguyen, T. X.; Bhatia, S. K.; Nicholson, D. *Langmuir* **2005**, *21*, 3187−3197.
(14) Jagiello, J.; Thommes, M. *Carbon* **2004**, *42*, 1227−1232.
(15) Peng, D.; Robinson, D. B. *Ind. Eng. Chem. Fundam.* **1976**, *15*, 59−64.
(16) Lastoskie, C.; Gubbins, K. E.; Quirke, N. *J. Phys. Chem.* **1993**, *97*, 4786−4796.
(17) Steele, W. A. *The Interaction of Gases with Solid Surfaces*; Pergamon: Oxford, 1974.
(18) Stan, G.; Cole, M. W. *J. Low Temp. Phys.* **1998**, *110*, 539.
(19) Silvera, I. F.; Goldman, V. V. *J. Chem. Phys.* **1978**, *69*, 4209.
(20) Kruk, M.; Li, Z.; Jaroniec, M.; Betz, W. R. *Langmuir* **1999**, *15*, 1435−1441.
(21) Lippens, B. C.; de Boer, J. H. *J. Catal.* **1965**, *4*, 319.
(22) Everett, D. H.; Powl, J. C. *J. Chem. Soc., Faraday Trans. 1* **1976**, *72*, 619.
(23) Wang, Q.; Johnson, J. K. *J. Chem. Phys.* **1999**, *110*, 577−586.
(24) Jagiello, J. *Langmuir* **1994**, *10*, 2778−2785.
(25) Jagiello, J.; Tolles, D. In *Fundamentals of Adsorption − FOA6*; Meunier, F., Ed.; Elsevier: Paris, 1998; pp 629−634.